



HAL
open science

Characterization of the glycosidic linkage of underivatized disaccharides by interaction with Pb^{2+} ions

Ahlam El Firdoussi, Marie Lafitte, Jeanine Tortajada, Omar Kone, Jean-Yves Salpin

► **To cite this version:**

Ahlam El Firdoussi, Marie Lafitte, Jeanine Tortajada, Omar Kone, Jean-Yves Salpin. Characterization of the glycosidic linkage of underivatized disaccharides by interaction with Pb^{2+} ions. *Journal of Mass Spectrometry*, 2007, 42 (8), pp.999-1011. 10.1002/jms.1220 . hal-00137575

HAL Id: hal-00137575

<https://hal.science/hal-00137575>

Submitted on 8 Oct 2018

HAL is a multi-disciplinary open access archive for the deposit and dissemination of scientific research documents, whether they are published or not. The documents may come from teaching and research institutions in France or abroad, or from public or private research centers.

L'archive ouverte pluridisciplinaire **HAL**, est destinée au dépôt et à la diffusion de documents scientifiques de niveau recherche, publiés ou non, émanant des établissements d'enseignement et de recherche français ou étrangers, des laboratoires publics ou privés.

Characterization of the glycosidic linkage of underivatized disaccharides by interaction with Pb²⁺ ions.

Ahlam El Firdoussi, Marie Lafitte, Jeanine Tortajada, Omar Kone and Jean-Yves Salpin*

Université d'Evry Val d'Essonne - Laboratoire Analyse et Modélisation pour la Biologie et l'Environnement, UMR CNRS 8587, Bâtiment Maupertuis, Boulevard François Mitterrand, 91025 EVRY CEDEX, France.

Corresponding author: Jean-Yves Salpin

Tel: 33 1 69 47 76 47 Fax: 33 1 69 47 76 55

e-mail : jean-yves.salpin@univ-evry.fr

Number of pages (including Table, Figures and schemes) : 30

Abstract Electrospray ionization in combination with tandem mass spectrometry and lead cationization is used to characterize the linkage position of underivatized disaccharides. Lead(II) ions react mainly with disaccharides by proton abstraction to generate [Pb(disaccharide)_m-H]⁺ ions (m=1-2). At low cone voltage, an intense series of doubly charged ions of general formula [Pb(disaccharide)_n]²⁺ are also observed. Our study shows that MS/MS experiments have to be performed to differentiate Pb²⁺-coordinated disaccharides. Upon collision, [Pb(disaccharide)-H]⁺ species mainly dissociate according to glycosidic bond cleavage and cross-ring cleavages leading to the elimination of C_nH_{2n}O_n neutrals (n=2-4). The various fragmentation processes allow the position of the glycosidic bond to be unambiguously located. Distinction between glc-glc and glc-fru disaccharides appears also straightforward. Furthermore, for homodimers of *D*-glucose our data demonstrate that the anomericity of the glycosidic bond can be characterized for the 1→*n* linkages (n=2,4,6). Consequently, Pb²⁺ cationization combined with tandem mass spectrometry therefore appears particularly useful to identify underivatized disaccharides.

KEYWORDS: Electrospray ionization, Lead(II) cationization, disaccharides, MS/MS experiments, glycosidic bond configuration

INTRODUCTION

Carbohydrates are mainly found as polysaccharides that play a crucial role in both animal and vegetal life. Cellulose for example, is a structural component of vegetal cell walls, whereas starch or glycogen act as food storage materials. These three polysaccharides are homopolymers of *D*-glucose and it turns out that both the role and the structure of these three macromolecules vary according to the nature of the glycosidic bonds. This clearly illustrates the fantastic diversity of carbohydrate chemistry.

Such a variety makes oligosaccharide analysis a tedious task for mass spectrometry. A complete structural description of carbohydrates implies notably exact mass measurement, sites and anomeric configuration of the glycosidic linkages, and stereochemical characterization of the different asymmetric centers of the sugar rings. However, as partial hydrolysis or enzymatic attack can be used to reduce the molecular weight of polysaccharides, the structure of the macromolecules can be deduced from that of smaller oligosaccharides such as mono- or disaccharides produced in the partial degradation. Consequently, many studies devoted to the characterization of isomeric mono- or disaccharides have been published in the literature during these past twenty years. Furthermore, the use of mass spectrometry for the determination of the linkage position between monosaccharide units has increased considerably with the advent of ionization techniques such Fast Atom Bombardment (FAB), Liquid Secondary Ion Mass Spectrometry (LSIMS), Matrix Assisted Laser Desorption Ionization mass spectrometry (MALDI), and Electrospray ionization (ESI). Linkage determination requires the reducing ring to be broken to provide structurally informative fragments. This can be easily achieved in the negative ion mode through in source or collision activated fragmentation of [saccharide-H]⁻ ions, regardless of the ionization technique used.¹⁻¹⁴ The peculiarity of the negative ionization is commonly proposed to consist in

a selective deprotonation of the anomeric hydroxyl (reducing end) which is more acidic with respect to the remaining acidic groups.^{15,16} A recent theoretical study about deprotonated disaccharides also suggests that the deprotonation of the C(2) hydroxyl of the non-reducing ring may play a key role for disaccharide fragmentation.¹⁷

Concerning the positive-ion mode, it has been shown¹⁸⁻²⁰ that mass spectra of protonated carbohydrates appear to be very useful for the determination of the molecular weight of underivatized oligosaccharides (intense molecular ion). Cleavages along the glycosidic bond and associated sequence information may be also obtained through protonation of the interglycosidic oxygen. However, as protonation does not induce fragmentation of the reducing ring, linkage information is hardly obtained. One can get around this problem by using of metallic salts as ionization agent. This approach has been greatly simplified thanks to the advent of the soft ionization techniques and especially electrospray. Metallic salts have been already successfully applied to characterize the various stereocenters of both derivatized and underivatized monosaccharides²⁰⁻³¹ because their particular reactivity induces extensive cross-ring cleavages. Alkali, alkaline earth and transition metal ions have been also used to determine the linkage position within oligosaccharides, the discrimination among the different types of linkage being based on either thermochemistry³², ion mobility^{33,34}, Kinetic Energy Release (KER) examination³⁵ or fragmentation through conventional CID^{20,36-49} or IRMPD^{50,51} experiments. Based on our results obtained with monosaccharides which emphasized the analytical potential of lead cationization under electrospray conditions³¹, the present paper aims to apply this methodology to the discrimination of the 1→n (n=1-6) glycosidic linkage. To this purpose, we have chosen a series of 15 disaccharides whose description is given in Table 1. This set of molecules will allow us to address the following points : i) characterization of the various glycosidic linkages for the glc-glc and glc-fru saccharides, ii) differentiation of the

stereochemistry of the glycosidic bond, iii) ketose/aldose distinction of the reducing end unit. Experiments have been carried out without any preliminary derivatization.

EXPERIMENTAL

Electrospray mass spectra were recorded on an Applied Biosystems/MDS Sciex API2000 triple-quadrupole instrument fitted with a "turboionspray" ion source. Solutions of Lead nitrate/disaccharide at various concentrations were prepared in pure water (purified with a Milli-Q water purification system) and were introduced in the source using direct infusion with a syringe pump, at a flow rate of 5 $\mu\text{L}/\text{min}$. Ionization of the samples was achieved by applying a voltage of 5.5 kV on the sprayer probe and by the use of a nebulizing gas (GAS1, air) surrounding the sprayer probe, intersected by a heated gas (GAS2, air) at an angle of approximately 90°. The operating pressure of GAS1 and GAS2 are adjusted to 2.1 bars, by means of an electronic board (pressure sensors), as a fraction of the air inlet pressure. The curtain gas (N_2), which prevents air or solvent from entering the analyzer region, was similarly adjusted to a value of 1.4 bars. The temperature of GAS2 was set at 100°C.

MS/MS spectra were carried out by introducing nitrogen as collision gas in the second quadrupole at a total pressure of 3×10^{-5} mbar, the background pressure being around 10^{-5} mbar. As detailed later, the declustering potential (DP), defined as the difference of potentials between the orifice plate and the skimmer (grounded), and typically referred to as the "cone voltage" for other electrospray interfaces, was fixed to 20 V to perform MS/MS experiments. Furthermore, MS/MS spectra were systematically recorded at different collision energies (the kinetic energy of ions is given by the difference of potentials between the focusing quadrupole Q0 preceding Q1, and the collision cell Q2). Lead nitrate was chosen because of its high solubility in water. All the disaccharides were dissolved in water without any preliminary derivatization. A 1:2 metal:sugar ratio was adopted based on our previous observations with monosaccharides.³¹ The resulting

pH of our aqueous mixtures of lead nitrate/disaccharide (5×10^{-5} mol.L⁻¹/ 10^{-4} mol.L⁻¹) is about 5, similar to that of Milli-Q water. Nevertheless, we made several experiments with a 50/50 (v:v) water/methanol mixture and we also observed intense lead/sugar complexes. However, spectra are more complicated because of additional complexation processes between lead and one or several molecules of methanol. Fortunately, these processes do not alter the mass region of the lead/sugar complex chosen for fragmentation. Moreover, MS/MS experiments have shown that CID spectra of those complexes are not solvent-dependent. It is therefore possible to carry out this study in a water/methanol mixture without using the heated drying gas.

Unless otherwise noted, mass to charge ratios mentioned throughout this paper refer to as peaks which include the most abundant Lead isotope (²⁰⁸Pb). Lead nitrate and all the disaccharides but *D*-gentiobiose (Interchim) were purchased from Aldrich Sigma and Fluka, and were used without further purification. 1-¹³C-*D*-cellobiose was purchased from Omicron biochemicals.

RESULTS AND DISCUSSION

Positive ion electrospray spectra of Lead nitrate/disaccharide mixture

Figure 1 presents the m/z 200-1500 range of the electrospray spectrum obtained at a declustering potential of 20 volts, when introducing an aqueous lead nitrate/*D*-laminaribiose mixture (5×10^{-5} mol.L⁻¹/ 10^{-4} mol.L⁻¹). As expected, peaks involving one lead atom are easily recognizable due to the characteristic isotopic pattern of this metal. Several types of ions are observed. The first one corresponds to hydrated lead hydroxide ions $\text{PbOH}^+ \cdot x\text{H}_2\text{O}$ ($x=0-5$ at m/z 225, 243, 261 279 and 297, 315) as confirmed by low-energy CID spectra. Increasing the declustering potential up to 200 Volts results in the gradual removal of these ions by successive losses of water. Note that a singly charged bare lead ion Pb^+ (m/z 208), starts to appear at DP=50 Volts, to become the base peak at

the highest DP. The protonated form of the disaccharide (m/z 343) is generally observed in low abundance. Like for monosaccharides^{31,52}, the interaction between the metal cation and the sugar results in the formation of singly charged ions, $[\text{Pb}(\text{D-disaccharide})_m - \text{H}]^+$ ($m=1,2$), detected at m/z 549 and 891. We also observe a nice series of doubly charged complexes of general formula $[\text{Pb}(\text{disaccharide})_n]^{2+}$ ions ($n=1-8$), at m/z 275, 446, 617, 788, 959, 1130, 1301 and 1472; Figure 1). The detection of these doubly charged species confirms the presence of Pb^{2+} ions in the aqueous solution, as already shown by Perera et al.⁵³ It is also worth mentioning that it is the first time during our studies about the interaction of lead with carbohydrates that we managed to detect with our instrument a doubly charged complex in which the metallic center interacts with a single and intact molecule (m/z 275). As already observed before by Stace and co-workers for $\text{Pb}(\text{ROH})_4^{2+}$ species ($\text{R}=\text{H}$, alkyl chains)⁵⁴, increasing the size and polarisability of the ligand results in the softening of the base and stabilization of the complex. While we did not succeed to detect such an ion with monosaccharides, a disaccharide turns to be a sufficiently big and polarizable ligand to stabilize the charge +2.

MS/MS spectra of the doubly-charged complexes

The MS/MS spectra of $[\text{Pb}(\text{D-nigerose})_n]^{2+}$ ($n=1-4$) are presented in Figure 2, all the spectra being recorded at a collision energy of 10 eV (laboratory frame), and with the poorest quadrupole resolution in order to gain in sensitivity. Using the lowest resolving power during mass selection is also particularly helpful in interpreting these MS/MS spectra since the peaks involving the metallic center present some kind of isotopic distribution and are consequently easily recognizable (for example m/z 327 in Figure 2a). Figure 2a shows that the smallest doubly charged ion (m/z 275) dissociates according to a heterolytic bond cleavage at the glycosidic oxygen thereby producing the

dehydroglucose cation (m/z 163) and a m/z 387 ion that may correspond to a complex between Pb^{2+} and a deprotonated form of *D*-glucose. Such a fragmentation has been already observed on MS/MS spectra of $[\text{M}(\text{mannotriose})]^{2+}$ species ($\text{M}=\text{Mn}$ or Co).⁴⁴ The dehydroglucose cation further dissociates by successive losses of water to produce m/z 145 and 127, while the m/z 97 and 85 ions probably correspond to elimination of CH_2O and $\text{C}_2\text{H}_4\text{O}_2$ from m/z 127 and 145, respectively. As for the metal alkoxide ion, it undergoes several competitive/successive fragmentation processes (loss of water and/or cross ring cleavage) to generate all the ions detected between above m/z 200, except for m/z 257, 239 and 221, that may correspond to the successive elimination of one, two or three molecules of water, respectively, from the precursor ion. Note that the m/z 369 ion is not observed on the MS/MS spectrum of $[\text{Pb}(\text{D-glucose})-\text{H}]^+$.⁵² consequently, one cannot definitely rule out the formation of this ion by a direct elimination of protonated *D*-glucose from the precursor ion, even if this latter ion is not detected.

The behavior of the doubly charged complexes is significantly different when $n \geq 2$. Examination of Figure 2b ($n=2$) indicates that the heterolytic cleavage leading to the dehydroglucose cation (m/z 163) is no longer observed since a complementary ion at m/z 729 would be detected. Instead, one can observe a dissociative proton transfer within the complex, giving rise to a $[\text{Pb}(\text{disaccharide})-\text{H}]^+$ ions (m/z 549). The complementary ion at m/z 343 is not detected but we may reasonably assume that this species is transiently generated and has enough internal energy to immediately lose either a molecule of water to form the ion at m/z 325, or a dehydroglucose moiety via a glycosidic bond cleavage to give the protonated *D*-glucose (m/z 181). This assumption is supported by the presence of the $(\text{disaccharide})\text{H}^+$ ion when Pb^{2+} interacts with 3 or 4 disaccharides (Figure 2c and 2d). These two ions further dissociate to give the ions detected at m/z 85, 97, 127, 145, 163 and 289. In looking at the high measured end of this spectrum, we can see that the $[\text{Pb}(\text{disaccharide})-\text{H}]^+$ complex also dissociates

according to various processes (elimination of water/cross-ring and glycosidic bond cleavages) giving rise to numerous fragments between m/z 225 and 531.

When a third nigerose unit interacts with the metal (Figure 2c), the dissociative proton transfer leading to $[\text{Pb}(\text{disaccharide})_2\text{-H}]^+$ (m/z 891) and $(\text{disaccharide})\text{H}^+$ (m/z 343) ions, competes with the elimination of an intact disaccharide unit and the concomitant formation of the doubly charged ion at m/z 446. Furthermore, successive eliminations of two disaccharides (m/z 788 \rightarrow m/z 617 \rightarrow m/z 446) are observed in Figure 2d. This result therefore suggests that Pb^{2+} ions may interact directly with two disaccharides in a first coordination shell, surrounded by the other disaccharide units via intermolecular hydrogen bonds (outer coordination sphere). The $[\text{Pb}(\text{disaccharide})_2\text{-H}]^+$ species gives rise to the $[\text{Pb}(\text{disaccharide})\text{-H}]^+$ complex (as confirmed by its MS/MS spectrum), which in turns dissociates as previously described. Note that the lack of $[\text{Pb}(\text{disaccharide})_m\text{-H}]^+$ ($m>2$) in Figure 2d is in agreement with a structure involving two coordination shells. Finally, ions at m/z 487 and 649 are also detected. Their origin is unclear. However, these ions do not include the metal and formally correspond to successive 162 Daltons increments from m/z 325. Further experiments beyond the scope of this report are necessary to postulate a mechanism for their formation.

Charge separation processes therefore constitute one possible way of formation of the $[\text{Pb}(\text{D-disaccharide})_m - \text{H}]^+$ species. We have carried out a declustering potential optimization by ramping its value from 0 to 200 volts. Our results show that the highest abundance for both singly and doubly charged complexes occurred at a DP of 20 Volts. Their intensity then dropped quickly above 30 volts. Indeed, raising the DP value induces dissociation of the different organometallic complexes. Finally, note that the presence of $[\text{Pb}(\text{D-disaccharide})_m - \text{H}]\cdot\text{HNO}_3^+$ ions at m/z 611 and 953 on the electrospray spectrum (Figure 1) suggests that the $[\text{Pb}(\text{D-disaccharide})_m - \text{H}]^+$ ions may be also formed by a proton transfer reaction between disaccharides and PbNO_3^+ .

We checked if "in-source" fragmentations induced by high skimmer voltage could be helpful for isomeric distinction. Unfortunately, isobaric disaccharides gave similar dissociations as the DP increased. Consequently, MS/MS experiments are required to differentiate the various isomers. For this purpose, we chose the $[\text{Pb}(\text{disaccharide})-\text{H}]^+$ species since it is the most intense complex detected for all the molecules studied. A 1:2 metal:monosaccharide ratio and a DP value of 20 volts were used for MS/MS experiments. The results are presented in the next section.

Low-energy CID spectra of $[\text{Pb}(\text{disaccharide})-\text{H}]^+$ ions

The different $[\text{Pb}(\text{disaccharide})-\text{H}]^+$ species involving ^{208}Pb (m/z 549) were selected and allowed to dissociate upon collision with nitrogen. For the sake of comparison, all the MS/MS spectra presented thereafter were recorded with strictly the same experimental conditions (gases, potentials), except for the collision energy, optimized for each compound so as to adjust the remaining intensity of the precursor ion to c.a. 25%. This results in center of mass collision energy ranging from 1 to 1.7 eV. The abundance of the various product ions are summarized in Table 1. Efforts were made to check the reproducibility of the MS/MS spectra. To this end, we recorded for each compound, a series of ten distinct product ion spectra. The standard deviations obtained are given in Table 1. We can see that they are systematically less than 5% of the most intense product ion for a given spectrum. Consequently, the product ion spectra appear sufficiently reproducible for confident use of abundance ratios of fragment ions if necessary.

The MS/MS spectra of the $[\text{Pb}(\text{disaccharide})-\text{H}]^+$ species are characterized by three kinds of ions. The first one corresponds to cross ring cleavages associated with elimination of $\text{C}_n\text{H}_{2n}\text{O}_n$ molecules ($n=2-4$) and formation of the m/z 489, 459 and 429 ions. The second one involves the breaking of the glycosidic linkage, giving rise to a couple of fragments at m/z 387 and 369. Finally, these glycosidic cleavage ions undergo

subsequent dissociations leading to numerous fragments in the m/z 200-387 range. Note that elimination of water from the precursor ion and producing an ion at m/z 531, is rarely observed independently of the linkage position, while it is one of the main fragmentation observed in the negative ion mode, but also for both protonated^{18,19} and Li- or Na-cationized ($1\rightarrow n$; $n=3,4,6$) disaccharides.^{20,36,37,43} Given the number of isomers considered, results will be organized according to three distinct sections.

Homodimers of D-glucose. The data obtained for the ten α and β isomeric glucose disaccharides are gathered in Table 1. The spectra recorded for isomeric α - $1\rightarrow n$ disaccharides are also given in Figure 3. Examination of this figure shows that the pattern of product ions is different for each different type of linkage, regardless the anomeric configuration of the non-reducing end, thus demonstrating the ability of lead cationisation for establishing the linkage position in homodimers of *D*-glucose. The fragments originating from cross-ring cleavage reactions (m/z 429, 459 and 489) indeed directly provide determination of the glycosidic bond type. Each glycosidic linkage is characterized by a specific combination of these fragments. Interestingly, these combinations are in agreement with those observed not only with alkali metals^{36,37,43,49} but also in the negative ion mode.^{8,9} These cross-ring cleavages occur very likely at the reducing ring since the ten isomers exhibit the same non-reducing end (glucose). Moreover, reducing ring fragmentation has been already established in a previous study by means of labelling experiments.³⁷

MS/MS spectra of the two *D*-trehalose isomers are characterized by a total lack of $C_nH_{2n}O_n$ elimination (Figure 3a). The MS/MS spectra are dominated by an intense peak at m/z 327, which comes from the m/z 387 species by elimination of a $C_2H_4O_2$ unit. Direct formation of m/z 327 from the precursor ion is proposed for 1,2-disaccharides (see Figure 3b), since their CID spectra exhibit an intense m/z 327 ion without any m/z 387, even at low collision energy. This dissociation corresponds to a $^{0,2}A_2$ cleavage. A

mechanism now commonly adopted for this particular fragmentation and based on ^{18}O -labelling^{36,37,55,56} and/or methylation studies⁵⁶, is initiated by migration of the proton of the anomeric hydroxyl and involves in a second step migration of the C(3) hydroxyl proton (Scheme 1).

<Scheme 1>

Our results give further support to this mechanism since the $^{0,2}\text{A}_2$ cleavage is not observed for 1,3-disaccharides. Furthermore, our detailed study about the interaction of Pb^{2+} ions with *D*-glucose⁵² has demonstrated that formation of $[\text{Pb}(\text{saccharide})\text{-H}]^+$ ion should rather involve deprotonation of the hydroxymethyl group, even if selective deprotonation of the anomeric hydroxyl, which is the more acidic group¹⁶ should be expected.

The second important dissociation process observed on MS/MS spectra is cleavage of the glycosidic bond leading to ions at m/z 387 and 369. It is worth noting that our previous study on *D*-glucose has shown that the m/z 369 ion cannot come from m/z 387 by loss of water. Due to the symmetry of the disaccharides, these two ions may be formed by cleavage of the glycosidic bond on either side of the bridging oxygen atom with metal attached on either side (Scheme 2), but in all cases leaving the bridging oxygen atom with the product ion.

<Scheme 2>

Cleavage of the C(1')-O(n) bond generates Y_1 and B_1 ions while formation of C_1 and Z_1 ions corresponds to cleavage of the C(n)-O(n) bond. Through ^{18}O -labelling of the anomeric oxygen on the reducing ring of *D*-gentiobiose and *D*-cellobiose, it was previously shown that there was only one glycosidic cleavage for Li ^{37,43} and Na -cationized⁴³ disaccharides, leading exclusively to Y_1 and B_1 ions. It has been also

suggested during a study about sodium-cationized *O*-methylated maltooligosaccharides⁵⁶ that since Z but not B ions still has a reducing end, cross-ring cleavages would be only expected for a MS³ of a Z fragment. We performed for the various disaccharides the MS/MS spectrum of the ion m/z 369 generated in the interface by "in-source" fragmentations. The results turned to be not conclusive, an ion at m/z 309 (loss of C₂H₄O₂ moiety) being not systematically detected. Furthermore, the reactivity of Pb²⁺ is hardly comparable to that of Na⁺ cation. In order to gain some insight about the identity of m/z 387 and 369, we recorded the MS/MS spectrum of the [Pb(1-¹³C^R-*D*-cellobiose)-H]⁺ ion (m/z 550, R meaning that the molecule is labelled on the reducing end). The spectrum (Figure 4) provides useful information. First, it demonstrates that the cross-ring cleavages indeed occur at the reducing ring, as attested by the losses of 61 and 121 Daltons from the precursor ion. Furthermore, the m/z ratios of ions m/z 387 and 369 appears not shifted, thus indicating that these ions would exclusively correspond to C₁ and B₁ respectively. Consequently, the two bridging bonds would be broken and the non-reducing unit would retain the metal. This result was quite unexpected because such reactivity has never been observed before with alkali metals. Note that for *D*-cellobiose, the ion at m/z 369 is also formed from the m/z 429 species by loss of C₂H₄O₂ (scheme 1). Two possible structures may be envisaged for this ion since previous studies have shown that migration of either oxygen-bonded or carbon-bonded H could be possible. A more detailed study involving ¹⁸O-labelling, extended to other disaccharides and combined with DFT calculations, is currently in progress in order to confirm the identity of the m/z 387 and 369 ions and to propose reliable mechanisms accounting for the observed product ions.

Characterization of heterodimers. In addition to homodimers of *D*-glucose, we have also studied a series of four α -1→*n*-glc-fru disaccharides (*n*=3-6). Among these molecules, *D*-leucrose (*n*=5) unambiguously exhibits a pyranosic *D*-fructose unit.

MS/MS spectra are given in Figure 5. Examination of the data shows that again the set of observed cross-ring cleavages allows an easy location of the glycosidic bond. The distinction appears to be more straightforward than that reported for protonated glc-fru disaccharides.¹⁸ For *D*-turanose and *D*-palatinose the overwhelming cross-ring fragment corresponds to the loss of 90 Daltons. The same was found in the negative-ion mode.⁵ MS/MS spectra are also characterized by a significant ion at m/z 387, corresponding either to Y_1 or C_1 ions. Although still isobaric, these two ions should be structurally different since they correspond to cationized *D*-fructose and *D*-glucose respectively. Our previous study about the structural characterization of hexoses³¹ has demonstrated that *D*-glucose and *D*-fructose could be easily distinguished by lead cationization. The MS/MS spectrum of the $[Pb(\text{monosaccharide})-H]^+$ ion exhibited an intense m/z 297 ion for *D*-fructose (base peak) while this ion is practically not detected for *D*-glucose. Conversely, the m/z 327 ion is characteristic of *D*-glucose (base peak). So, we recorded for the glc-fru disaccharides the MS/MS spectrum of the m/z 387 species. The spectra exhibit both the m/z 327 and 297 species, the latter being overwhelming. This suggests that unlike *D*-cellobiose, the ion at m/z 387 would correspond to a mixture of structures and that both Y_1 and C_1 could be generated, Y_1 being dominant. This result is consistent with the data reported for protonated glc-fru disaccharides.¹⁸ Complementary ¹⁸O-labelling experiments are necessary to confirm or rule out this assumption. From Table 1, one can also see that for a given glycosidic bond type, glc-glc and glc-fru disaccharides can be distinguished. For the α -1 \rightarrow 3 linkage (*D*-nigerose vs *D*-turanose), the base peak is different and the ion at m/z 279 is only observed for the homodimer. Concerning the α -1 \rightarrow 4 linkage (*D*-maltose/*D*-maltulose), the two isomers do exhibit neither the same base peak nor the same pattern of cross-ring cleavages. Finally, in the case of α -1 \rightarrow 6 linkage, the distinction is achieved thanks to the identity of the base peak.

Finally, we have also studied the cationization of β -D-lactose (β -1 \rightarrow 4 gal-glc) and compared its MS/MS spectrum to that of D-cellobiose. The distinction is not as straightforward as for glc-fru isomers, the two spectra globally presenting the same fragment ions. However, even if these spectra, at a first glance, are rather similar, they may be useful for analytical purpose, by considering the abundance ratio 387/369. These ratios are equal to 0.34 and 1.18 for D-cellobiose and β -D-lactose, respectively. These values are significantly different and we can conclude that lead cationization combined with tandem mass spectrometry, allows, under our experimental conditions, D-cellobiose and β -D-lactose to be distinguished.

Anomeric configuration of the glycosidic bond. While numerous mass spectrometry approaches have been devoted to the characterization of the linkage position, fewer studies have been carried out on the glycosidic configuration. In the negative ion mode, it has been shown that the MS/MS spectrum of the $[M-H]^-$ ion (m/z 341) of underivatized glucose disaccharides having the same linkage but different anomeric configuration, exhibit some differences. The most striking one is the relative abundance of the ion at m/z 221, which is consistently greater for the α -anomer than for the corresponding β -anomer, regardless of the ionization technique (FAB or electrospray).^{5,9} In their FAB study⁵, Dallinga and Heerma also used the CA spectrum of the m/z 221 ion to determine the linkage configuration. Very recently, an electrospray study by Fang et al. used the same approach.⁵⁷ Furthermore, these authors unambiguously demonstrated that the m/z 221 ion is comprised solely of an intact non-reducing sugar with a two-carbon aglycon derived from the reducing ring.

In the positive-ion mode, Smith and Leary have also used FAB to differentiate between the anomeric configuration for a series of glucopyranosyl disaccharides.³⁵ This was achieved on the basis of kinetic energy release (KER) measurements for the dissociation of the metastable ion $[Co(acac)_2/disaccharide]^+$ complex (acac : acetylacetate). The

combination of conventional CID experiments with cationization by lithium or sodium does not lead to a clear-cut characterization of the glycosidic configuration. However, the abundance ratio Y_1/B_1 ion was found higher for the α -glycosyl bonds.⁴³⁻⁴⁹ Note that lithium cationization has been recently combined with infrared multiple-photon dissociation (IR-MPD) involving a free electron laser (FEL).⁵¹ In contrast to the CID studies, variation in the wavelength of irradiation allowed to obtain two-dimensional infrared irradiation mass spectra, which differed markedly between anomers. However, the authors emphasized that in conventional FTICR instruments fitted with a commercial but non-tunable CO₂ laser, the fixed IR wavelength of 10.6 μm does not allow α - and β -anomers to be distinguished. As FEL are not widely accessible devices, there is still need for a simple methodology to establish the anomeric configuration in oligosaccharides. This could be obtained in the positive-ion mode by using other metal ions than Li⁺ or Na⁺. As a matter of fact, previous FAB studies have already addressed the mass spectrometric characterization of the C(1) stereocenter of 1-*O*-methyl-*D*-glucopyranosides by studying the unimolecular decompositions of [M-Ag]⁺ species.^{58,29} Similarly, we demonstrated^{29,31} that the reactivity of Lead(II) ions under electrospray conditions could allow to discriminate anomers of 1-*O*-methyl-*D*-glucose. Data obtained with the glucopyranosyl disaccharides are summarized in table 1 and are illustrated by Figure 6. These data lead to mixed results. Like for monosaccharides, the MS/MS spectra obtained for 1 \rightarrow 2, 1 \rightarrow 4 and 1 \rightarrow 6 isomers establish the ion at m/z 351 (formed by loss of water from m/z 369) as specific of the α anomericity. However, such a clear-cut distinction is not achieved for the 1 \rightarrow 1 linkage. Indeed, the MS/MS spectra are very similar and a peak at m/z 351 is not observed. Concerning the 1 \rightarrow 3 linkage, the peak at m/z 351 is significantly more intense for *D*-nigerose (α -anomer), but is also observed for *D*-sophorose (β -anomer). Consequently, the reactivity of Pb²⁺ ion appears to be not specific enough to characterize the

anomericity of the non-reducing ring for all the glycosidic linkages. Complementary experiments are currently in progress in order to determine if other metal ions could constitute the ideal tool for this purpose.

CONCLUSION

The present study has demonstrated that diastereomeric disaccharides could be distinguished using Lead cationization and electrospray/triple-quadrupole mass spectrometry, without any preliminary derivatization. More particularly, for a given anomeric configuration, linkage position can be easily characterized for both the glc-fru and glc-glc series by MS/MS experiments on $[\text{Pb}(\text{disaccharide})\text{-H}]^+$ complexes. The nature of the reducing ring (glucose or fructose) can also be easily determined. Concerning the stereochemistry of the glycosidic bond (anomericity of the non-reducing ring), a clear-cut distinction is achieved, but only for the 1→2, 1→4 and 1→6 linkages, a specific fragment ion (m/z 351) being solely detected for the α -anomers. A more detailed study involving ^{18}O -labelling extended to several disaccharides and combined with DFT calculations is currently in progress so as to suggest possible mechanisms of dissociation of the $[\text{Pb}(\text{disaccharide})\text{-H}]^+$ complexes, as well as the preferred coordination sites for Pb^{2+} ions.

References

1. Domon B, Costello CE. A Systematic Nomenclature for Carbohydrate Fragmentations in Fab-MS/MS Spectra of Glycoconjugates. *Glycoconjugate J.* 1988; **5**: 397.
2. Ballistreri A, Garozzo D, Montaudo G, Giuffrida M, Impallomeni G. Determination of linkage position in disaccharides by negative-ion fast atom bombardment mass spectrometry. *Rapid Commun. Mass Spectrom.* 1989; **3**: 302.
3. Garozzo D, Giuffrida M, Impallomeni G, Ballistreri A, Montaudo G. Determination of linkage position and identification of the reducing end in linear

- oligosaccharides by negative ion fast atom bombardment mass spectrometry. *Anal. Chem.* 1990; **62**: 279.
4. Garozzo D, Impallomeni G, Spina E, Green BN, Hutton T. Linkage Analysis in Disaccharides by Electrospray Mass Spectrometry. *Carbohydr. Res.* 1991; **221**: 253.
 5. Dallinga JW, Heerma W. Reaction mechanism and fragment ion structure determination of deprotonated small oligosaccharides, studied by negative ion fast atom bombardment (tandem) mass spectrometry. *Biol. Mass Spectrom.* 1991; **20**: 215.
 6. Lamb DJ, Wang HM, Mallis LM, Linhardt RJ. Negative-Ion Fast-Atom-Bombardment Tandem Mass-Spectrometry to Determine Sulfate and Linkage Position in Glycosaminoglycan-Derived Disaccharides. *J. Am. Soc. Mass Spectrom.* 1992; **3**: 797.
 7. Carroll JA, Ngoka L, Beggs CG, Lebrilla CB. Liquid secondary ion mass spectrometry Fourier transform mass spectrometry of oligosaccharide Anions. *Anal. Chem.* 1993; **65**: 1582.
 8. Carroll JA, Willard D, Lebrilla CB. Energetics of Cross-Ring Cleavages and Their Relevance to the Linkage Determination of Oligosaccharides. *Anal. Chim. Acta* 1995; **307**: 431.
 9. Mulroneo B, Traeger JC, Stone BA. Determination of Both Linkage Position and Anomeric Configuration in Underivatized Glucopyranosyl Disaccharides by Electrospray Mass-Spectrometry. *J. Mass Spectrom.* 1995; **30**: 1277.
 10. Perreault H, Costello CE. Stereochemical effects on the mass spectrometric behavior of native and derivatized trisaccharide isomers: Comparisons with results from molecular modeling. *J. Mass Spectrom.* 1999; **34**: 184.
 11. Desaire H, Leary JA. Detection and quantification of the sulfated disaccharides in chondroitin sulfate by electrospray tandem mass spectrometry. *J. Am. Soc. Mass Spectrom.* 2000; **11**: 916.
 12. Chai W, Piskarev V, Lawson AM. Negative-Ion electrospray mass spectrometry of neutral underivatized oligosaccharides. *Anal. Chem.* 2001; **73**: 651.
 13. Saad OM, Leary JA. Delineating mechanisms of dissociation for isomeric heparin disaccharides using isotope labeling and ion trap tandem mass spectrometry. *J. Am. Soc. Mass Spectrom.* 2004; **15**: 1274.
 14. Saad OM, Leary JA. Compositional analysis and quantification of heparin and heparan sulfate by electrospray ionization ion trap mass spectrometry. *Anal. Chem.* 2003; **75**: 2985.
 15. Mulroneo B, Peel JB, Traeger JC. Relative gas-phase acidities of glucopyranose from molecular orbital calculations. *J. Mass Spectrom.* 1999; **34**: 544.
 16. Salpin JY, Tortajada J. Gas-phase acidity of D-glucose. A density functional theory study. *J. Mass Spectrom.* 2004; **39**: 930.

17. Mulrone y B, Peel JB, Traeger JC. Theoretical study of deprotonated glucopyranosyl disaccharide fragmentation. *J. Mass Spectrom.* 1999; **34**: 856.
18. Dallinga JW, Heerma W. Positive ion fast atom bombardment mass spectrometry of some small oligosaccharides. *Biol. Mass Spectrom.* 1991; **20**: 99.
19. Zapfe S, Muller D. Unexpected gas-phase reactions of some underivatized disaccharides and of proton-bound dimers of monosaccharides by liquid-assisted secondary ion mass spectrometry. *Rapid Commun. Mass Spectrom.* 1998; **12**: 545.
20. March RE, Stadey CJ. A tandem mass spectrometric study of saccharides at high mass resolution. *Rapid Commun. Mass Spectrom.* 2005; **19**: 805.
21. Gaucher SP, Leary JA. Stereochemical differentiation of mannose, glucose, galactose, and talose using zinc(II) diethylenetriamine and ESI ion trap mass spectrometry. *Anal. Chem.* 1998; **70**: 3009.
22. Smith G, Leary JA. Synthesis and analysis of electrospray ionization-generated five-coordinate diastereomeric Ni-N-glycoside complexes using a quadrupole ion trap mass spectrometer. *Int. J. Mass Spectrom.* 1999; **193**: 153.
23. Smith G, Kaffashan A, Leary JA. Influence of coordination number and ligand size on the dissociation mechanisms of transition metal monosaccharide complexes. *Int. J. Mass Spectrom.* 1999; **183**: 299.
24. Desaire H, Leary JA. Multicomponent quantification of diastereomeric hexosamine monosaccharides using ion trap tandem mass spectrometry. *Anal. Chem.* 1999; **71**: 4142.
25. Desaire H, Leary JA. Differentiation of diastereomeric *N*-acetylhexosamine monosaccharides using ion trap tandem mass spectrometry. *Anal. Chem.* 1999; **71**: 1997.
26. Gaucher SP, Leary JA. Influence of metal ion and coordination geometry on the gas phase dissociation and stereochemical differentiation of *N*-glycosides. *Int. J. Mass Spectrom.* 2000; **197**: 139.
27. Carlesso V, Fournier F, Tabet JC. Stereochemical differentiation of four monosaccharides using transition metal complexes by electrospray ionization/ion-trap mass spectrometry. *Eur. J. Mass Spectrom.* 2000; **6**: 421.
28. Desaire H, Leary JA. The effects of coordination number and ligand size on the gas phase dissociation and stereochemical differentiation of cobalt-coordinated monosaccharides. *Int. J. Mass Spectrom.* 2001; **209**: 171.
29. Salpin JY, Boutreau L, Haldys V, Tortajada J. Gas-phase reactivity of glycosides and methyl glycosides with Cu⁺, Ag⁺ and Pb²⁺ ions by fast-atom bombardment and tandem mass spectrometry. *Eur. J. Mass Spectrom.* 2001; **7**: 321.

30. Carlesso V, Afonso C, Fournier F, Tabet JC. Stereochemical effects from doubly-charged iron clusters for the structural elucidation of diastereomeric monosaccharides using ESI/IT-MS. *Int. J. Mass Spectrom.* 2002; **219**: 559.
31. Salpin JY, Tortajada J. Structural characterization of hexoses and pentoses using lead cationization. An electrospray ionization and tandem mass spectrometric study. *J. Mass Spectrom.* 2002; **37**: 379.
32. Cerda BA, Wesdemiotis C. Thermochemistry and structures of Na⁺ coordinated mono- and disaccharide stereoisomers. *Int. J. Mass Spectrom.* 1999; **189**: 189.
33. Gabryelski W, Froese KL. Rapid and sensitive differentiation of anomers, linkage, and position isomers of disaccharides using High-Field Asymmetric Waveform Ion Mobility Spectrometry (FAIMS). *J. Am. Soc. Mass Spectrom.* 2003; **14**: 265.
34. Clowers BH, Dwivedi P, Steiner WE, Hill JHH, Bendiak B. Separation of Sodiated Isobaric Disaccharides and Trisaccharides Using Electrospray Ionization-Atmospheric Pressure Ion Mobility-Time of Flight Mass Spectrometry. *J. Am. Soc. Mass Spectrom.* 2005; **16**: 660.
35. Smith G, Leary JA. Differentiation of stereochemistry of glycosidic bond configuration: Tandem mass spectrometry of diastereomeric cobalt-glucosyl-glucose disaccharide complexes. *J. Am. Soc. Mass Spectrom.* 1996; **7**: 953.
36. Zhou ZR, Ogden S, Leary JA. Linkage Position Determination in Oligosaccharides - Ms/Ms Study of Lithium-Cationized Carbohydrates. *J. Org. Chem.* 1990; **55**: 5444.
37. Hofmeister GE, Zhou Z, Leary JA. Linkage Position Determination in Lithium-Cationized Disaccharides - Tandem Mass-Spectrometry and Semiempirical Calculations. *J. Am. Chem. Soc.* 1991; **113**: 5964.
38. Lemoine J, Fournet B, Despeyroux D, Jennings KR, Rosenberg R, Dehoffmann E. Collision-Induced Dissociation Of Alkali-Metal Cationized And Permethylated Oligosaccharides - Influence Of The Collision Energy And Of The Collision Gas For The Assignment Of Linkage Position. *J. Am. Soc. Mass Spectrom.* 1993; **4**: 197.
39. Fura A, Leary JA. Differentiation of Ca²⁺-Coordinated and Mg²⁺-Coordinated Branched Trisaccharide Isomers - an Electrospray-Ionization and Tandem Mass-Spectrometry Study. *Anal. Chem.* 1993; **65**: 2805.
40. Dongre AR, Wysocki VH. Linkage Position Determination of Lithium-Cationized Disaccharides by Surface-Induced Dissociation Tandem Mass-Spectrometry. *Org. Mass Spectrom.* 1994; **29**: 700.
41. Kovacik V, Hirsch J, Kovac P, Heerma W, Thomasoates J, Haverkamp J. Oligosaccharide Characterization Using Collision-Induced Dissociation Fast-Atom-Bombardment Mass-Spectrometry - Evidence for Internal Monosaccharide Residue Loss. *J. Mass Spectrom.* 1995; **30**: 949.
42. Cancilla MT, Penn SG, Carroll JA, Lebrilla CB. Coordination of alkali metals to oligosaccharides dictates fragmentation behavior in matrix assisted laser

- desorption ionization Fourier transform mass spectrometry. *J. Am. Chem. Soc.* 1996; **118**: 6736.
43. Asam MR, Glish GL. Tandem mass spectrometry of alkali cationized polysaccharides in a quadrupole ion trap. *J. Am. Soc. Mass Spectrom.* 1997; **8**: 987.
 44. Sible EM, Brimmer SP, Leary JA. Interaction of first row transition metals with alpha 1-3, alpha 1-6 mannotriose and conserved trimannosyl core oligosaccharides: A comparative electrospray ionization study of doubly and singly charged complexes. *J. Am. Soc. Mass Spectrom.* 1997; **8**: 32.
 45. Konig S, Leary JA. Evidence for linkage position determination in cobalt coordinated pentasaccharides using ion trap mass spectrometry. *J. Am. Soc. Mass Spectrom.* 1998; **9**: 1125.
 46. Leavell MD, Leary JA. Stabilization and linkage analysis of metal-ligated sialic acid containing oligosaccharides. *J. Am. Soc. Mass Spectrom.* 2001; **12**: 528.
 47. Xue J, Song LG, Khaja SD, Locke RD, West CM, Laine RA, Matta KL. Determination of linkage position and anomeric configuration in Hex-Fuc disaccharides using electrospray ionization tandem mass spectrometry. *Rapid Commun. Mass Spectrom.* 2004; **18**: 1947.
 48. Zhang J, Brodbelt JS. Silver Complexation and Tandem Mass Spectrometry for Differentiation of Isomeric Flavonoid Diglycosides. *Anal. Chem.* 2005; **77**: 1761.
 49. Yamagaki T, Fukui K, Tachibana K. Analysis of glycosyl bond cleavage and related isotope effects in collision-induced dissociation quadrupole-time-of-flight mass spectrometry of isomeric trehaloses. *Anal. Chem.* 2006; **78**: 1015.
 50. Xie YM, Lebrilla CB. Infrared multiphoton dissociation of alkali metal-coordinated oligosaccharides. *Anal. Chem.* 2003; **75**: 1590.
 51. Polfer NC, Valle JJ, Moore DT, Oomens J, Eyler JR, Bendiak B. Differentiation of isomers by wavelength-tunable infrared multiple-photon dissociation-mass spectrometry: Application to glucose-containing disaccharides. *Anal. Chem.* 2006; **78**: 670.
 52. Salpin JY, Tortajada J. Gas-phase reactivity of lead(II) ions with *D*-glucose. Combined electrospray ionization mass spectrometry and theoretical study. *J. Phys. Chem. A* 2003; **107**: 2943.
 53. Perera WN, Hefter G, Sipos PM. An investigation of the lead(II)-hydroxide system. *Inorganic Chemistry. Jul* 2001; **40**: 3974.
 54. Akibo-Betts G, Barran PE, Puskar L, Duncombe B, Cox H, Stace AJ. Stable $\text{Pb}(\text{ROH})_n^{2+}$ complexes in the gas phase: Softening the base to match the Lewis acid. *J. Am. Chem. Soc.* 2002; **124**: 9257.
 55. Friedl CH, Lochnit G, Geyer R, Karas M, Bahr U. Structural Elucidation of Zwitterionic Sugar Cores from Glycosphingolipids by Nanoelectrospray

- Ionization-Ion-Trap Mass Spectrometry. *Analytical Biochemistry* 2000; **284**: 279.
56. Tuting W, Adden R, Mischnick P. Fragmentation pattern of regioselectively O-methylated maltooligosaccharides in electrospray ionisation-mass spectrometry/collision induced dissociation. *Int. J. Mass Spectrom.* 2004; **232**: 107.
 57. Fang TT, Zirrolli J, Bendiak B. Differentiation of the anomeric configuration and ring form of glucosyl-glycolaldehyde anions in the gas phase by mass spectrometry: isomeric discrimination between m/z 221 anions derived from disaccharides and chemical synthesis of m/z 221 standards. *Carbohydr. Res.* 2007; **342**: 217.
 58. Berjeaud JM, Couderc F, Promé JC. Stereochemically controlled decomposition of silver-cationized methyl glycosides. *Org. Mass Spectrom.* 1993; **28**: 455.

Table and Figure caption

Table 1: Abundance (%) of the main fragment ions in the CID spectra of the [Pb(disaccharide)- H]⁺ ions (*m/z* 549)

Figure 1. *m/z* 200-800 range of the positive-ion electrospray mass spectrum of an aqueous Pb(NO₃)₂/*D*-laminaribiose (5 10⁻⁵ mol.L⁻¹/10⁻⁴ mol.L⁻¹) solution.

Figure 2. Low-energy CID spectra of [Pb(*D*-nigerose)_{*m*}]²⁺ ions with **a)** *m*=1 (*m/z* 275), **b)** *m*=2 (*m/z* 446), **c)** *m*=3 (*m/z* 617) and **d)** *m*=4 (*m/z* 788).

Figure 3. Low-energy CID spectra of [Pb(α -1 \rightarrow *n* glc-glc) - H]⁺ ions (*m/z* 549) with **a)** *n*=1, **b)** *n*=2, **c)** *n*=3, **d)** *n*=4 and **e)** *n*=6 .

Figure 4. MS/MS spectrum obtained with labelled *D*-cellobiose (1-¹³C^R-*D*-cellobiose, R meaning that the molecule is labelled on the reducing end)

Figure 5. Low-energy CID spectra of [Pb(α -1 \rightarrow *n* glc-fru) - H]⁺ ions (*m/z* 549) with **a)** *n*=3, **b)** *n*=4, **c)** *n*=5 and **d)** *n*=6 .

Figure 6. Characterization of the glycosidic configuration for 1 \rightarrow 6 glc-glc disaccharides.

Table 1: Abundance (%) of the main fragment ions in the CID spectra of the [Pb(disaccharide)- H]⁺ ions (m/z 549)^a.

Name	Type	Parent		Fragment ions									
		m/z 549	m/z 489	m/z 459	m/z 429	m/z 387	m/z 369	m/z 351	m/z 327	m/z 309	m/z 297	m/z 279	m/z 267
<i>D</i> -Trehalose	$\alpha\alpha$ -1→1 glc-glc	24.9±0.9				23.2±1.6	6.6±1.0		100	7.3±0.9	3.3±0.5	12.2±1.1	39.7±2.0
<i>D</i> -Neotrehalose	$\alpha\beta$ -1→1 glc-glc	25.6±0.9				42.4±1.8	5.3±0.4		100			3.1±0.2	13.2±0.7
<i>D</i> -Kojibiose	α -1→2 glc-glc	25.2±1.1			63.7±4.1		100	35.5±1.4	38.5±2.6	39.3±2.7	5.3±0.7	14.3±1.5	69.5±3.9
<i>D</i> -Sophorose	β -1→2 glc-glc	25.5±1.3			63.7±2.9		100	4.0±0.7	10.1±0.6	5.6±0.6	3.7±0.5	6.4±0.6	24.8±1.8
<i>D</i> -Nigerose	α -1→3 glc-glc	24.9±1.2		27.5±2.7	4.1±1.2	19.7±1.9	38.0±2.6	16.1±1.9	100	20.9±2.0	66.0±4.0	19.5±1.8	78.8±3.2
<i>D</i> -Turanose	α -1→3 glc-fru	24.8±0.9		100		17.9±0.6	31.7±0.8	7.5±0.3	38.0±0.7	4.6±0.2	34.8±1.4		10.4±0.5
<i>D</i> -Laminaribiose	β -1→3 glc-glc	24.6±1.0		9.6±1.1	21.3±0.8	11.0±1.2	97.0±2.8	5.3±0.8	89.3±5.4	17.3±2.1	33.1±3.6	35.2±4.6	100
<i>D</i> -Maltose	α -1→4 glc-glc	26.1±0.9	24.0±1.0		100	14.6±0.1	49.6±1.8	9.9±0.5	14.1±1.0	6.0±0.5	13.4±0.9		8.8±0.8
<i>D</i> -Maltulose	α -1→4 glc-fru	25.1±1.0		4.0±0.1	29.3±1.6	57.6±1.3	44.9±1.6	8.2±0.5	53.9±1.7	9.2±0.4	100	4.7±0.3	19.0±0.7
<i>D</i> -Cellobiose	β -1→4 glc-glc	26.0±1.2	14.5±0.7		100	19.4±0.7	57.9±1.9		31.8±1.2		6.7±0.6		7.3±0.8
β - <i>D</i> -Lactose	β -1→4 gal-glc	25.2±0.8	16.9±0.9	3.1±0.3	100	45.4±2.1	38.3±2.1		31.5±1.4		10.8±0.9	4.1±0.5	13.1±0.7
<i>D</i> -Leucrose	α -1→5 glc-fru	24.7±0.9		4.4±1.0	15.0±0.7	36.2±2.2	39.2±3.2	13.2±1.2	19.3±1.2	26.2±2.1	100	15.3±1.3	48.4±3.1
<i>D</i> -Palatinose	α -1→6 glc-fru	24.8±0.8	3.0±0.3	78.4±2.8	18.3±1.2	3.4±0.4	78.3±3.4	31.9±1.8	12.0±0.7	7.4±0.6	100	15.4±0.7	84.5±3.1
<i>D</i> -Isomaltose	α -1→6 glc-glc	24.8±0.8	29.7±3.1	34.9±3.2	85.4±4.3	6.4±1.4	100	35.1±1.6	27.5±3.0	36.6±3.9	36.3±1.5	13.4±1.3	57.8±5.4
<i>D</i> -Gentiobiose	β -1→6 glc-glc	24.8±0.8	24.8±1.6	9.6±1.0	66.8±3.3	4.4±0.6	100		15.7±0.7		3.3±0.4	5.9±0.7	13.1±0.7

^aThe percentages are expressed relative to the most abundant fragment. Peaks whose relative intensities are below 3% have not been taken into account

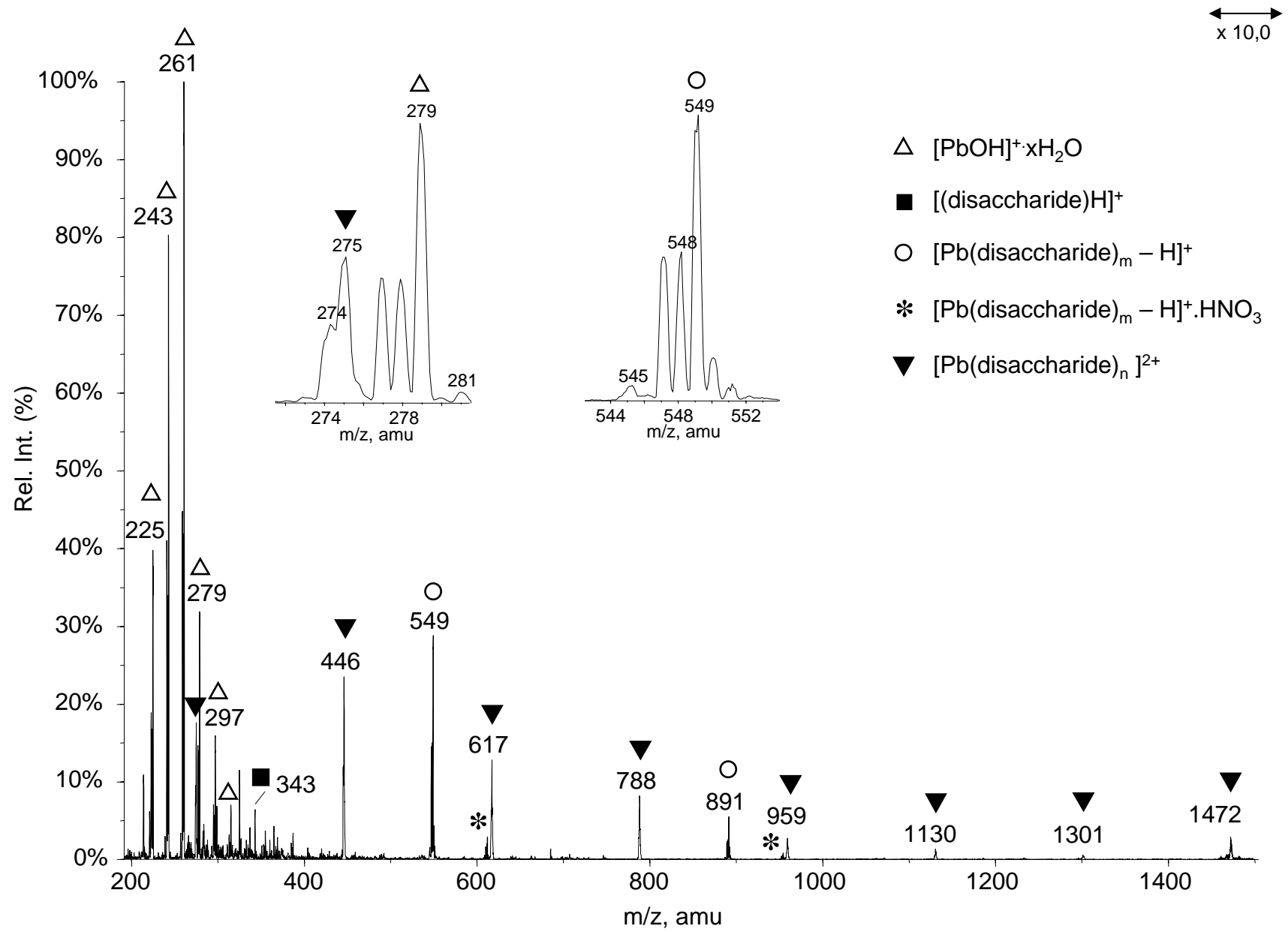


Figure 1

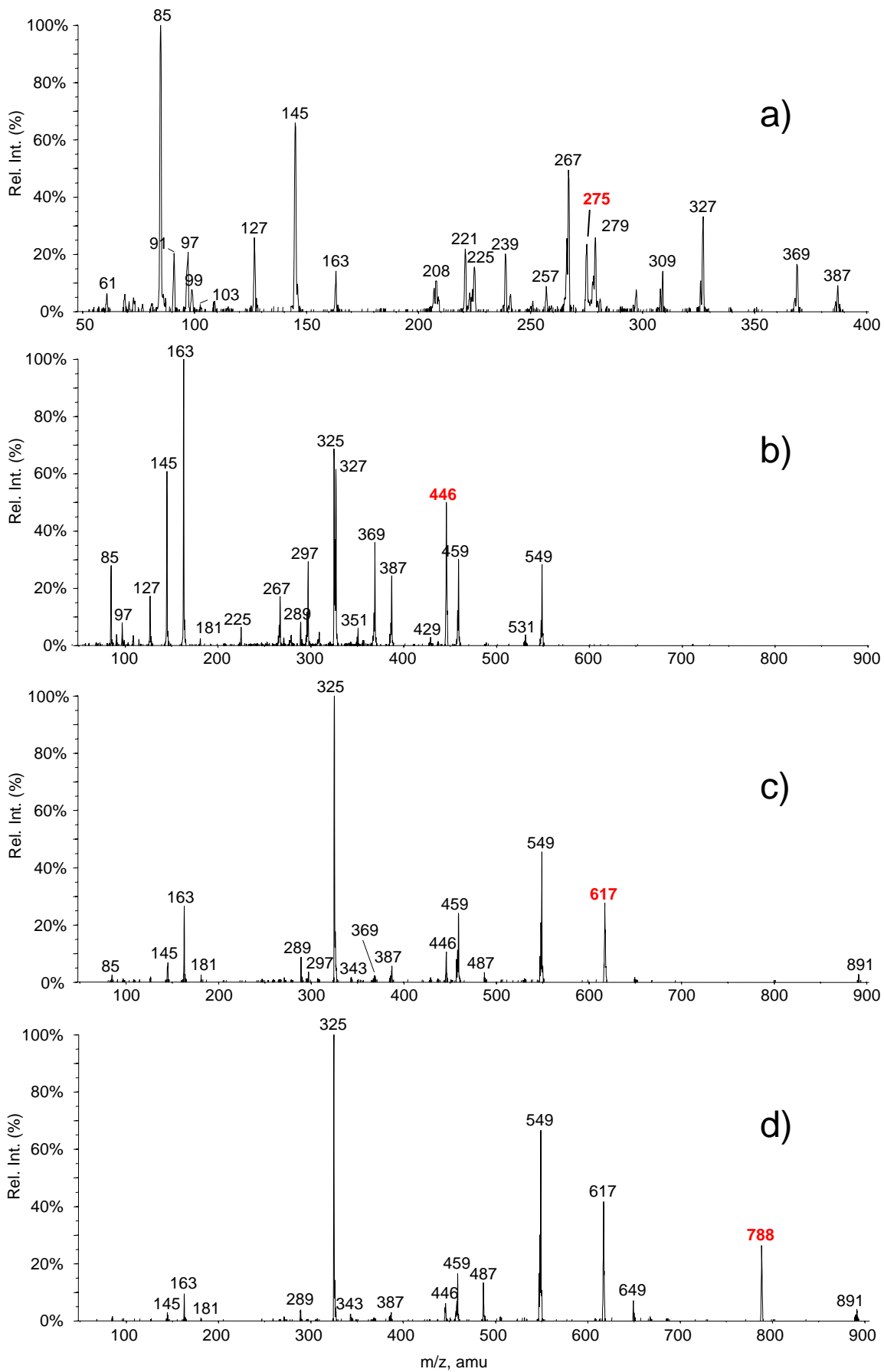


Figure 2

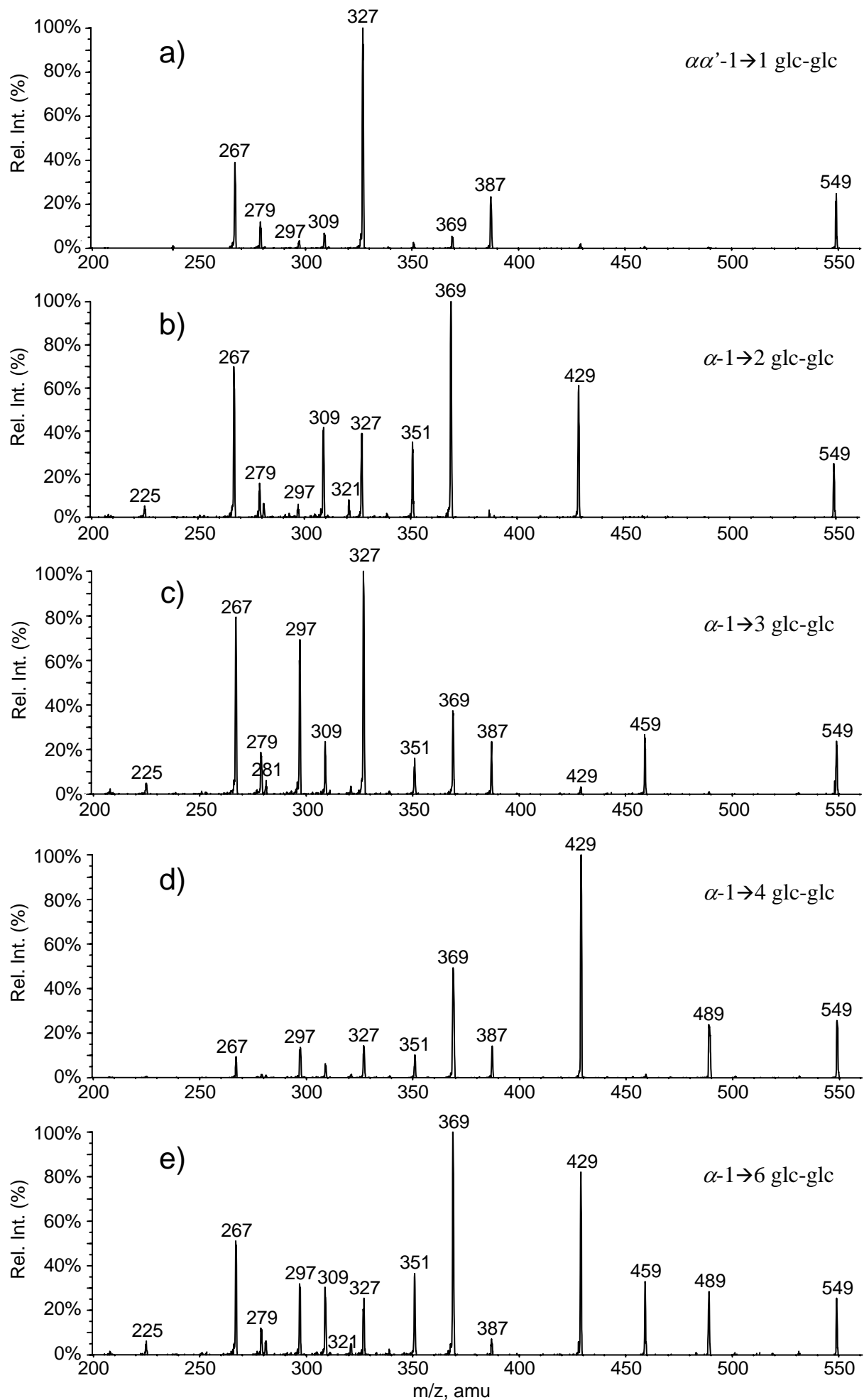


Figure 3

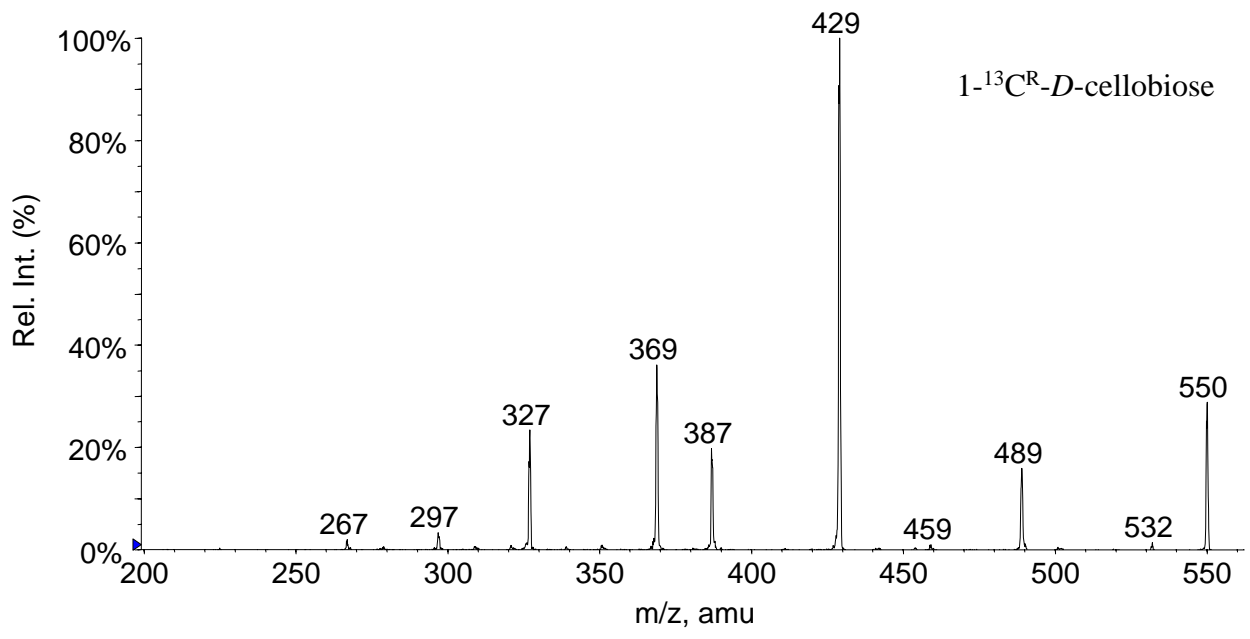


Figure 4

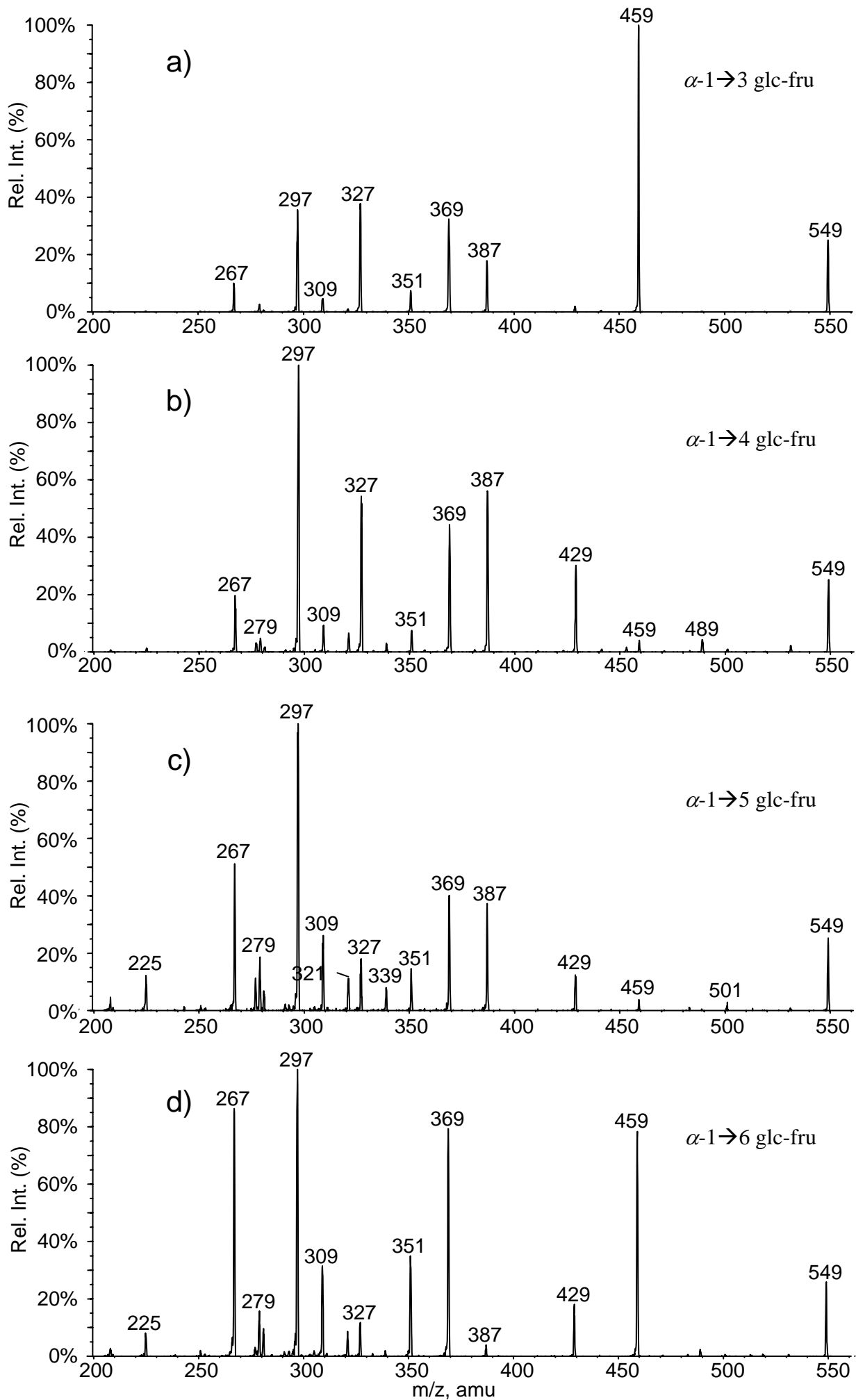


Figure 5

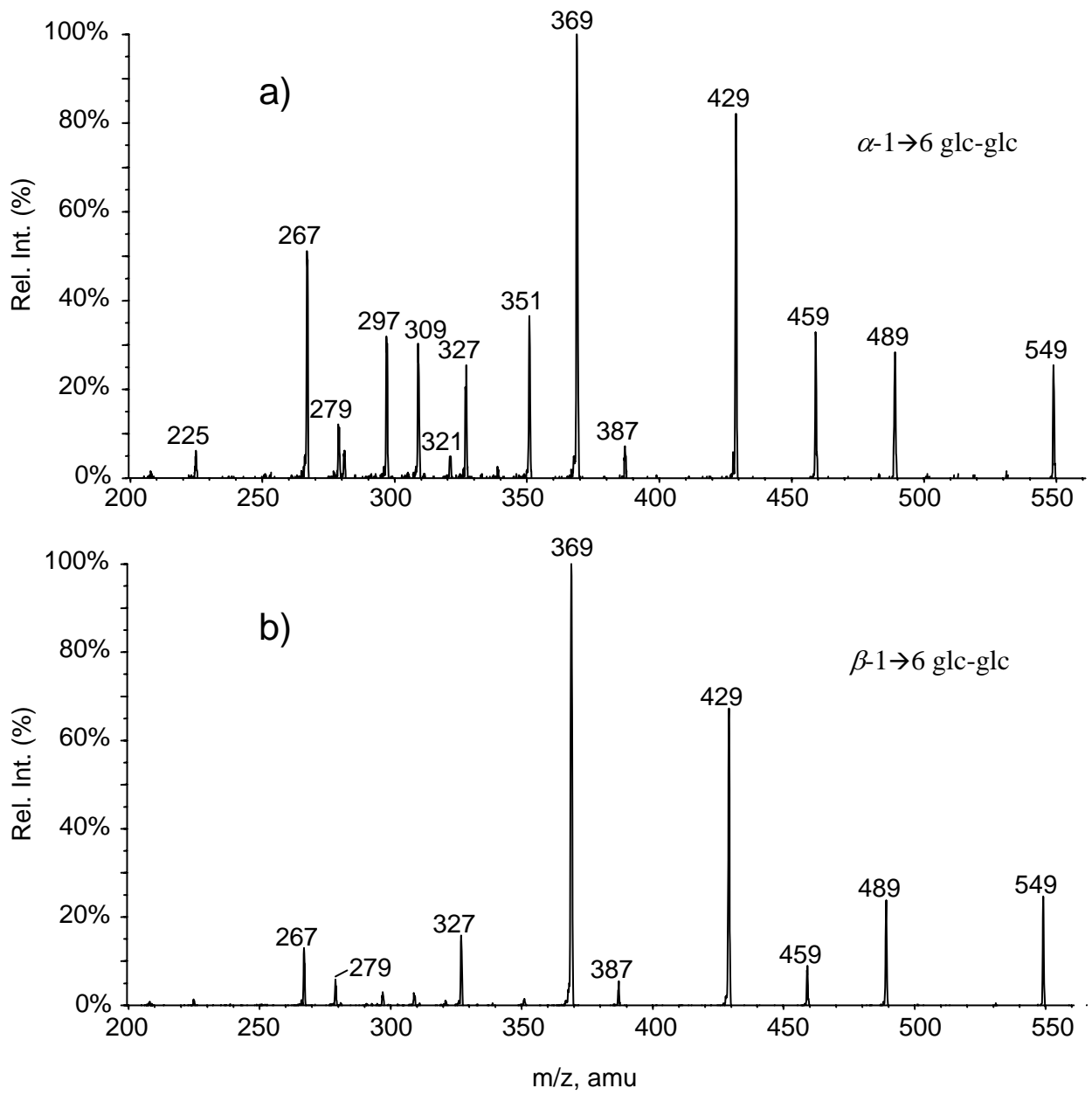
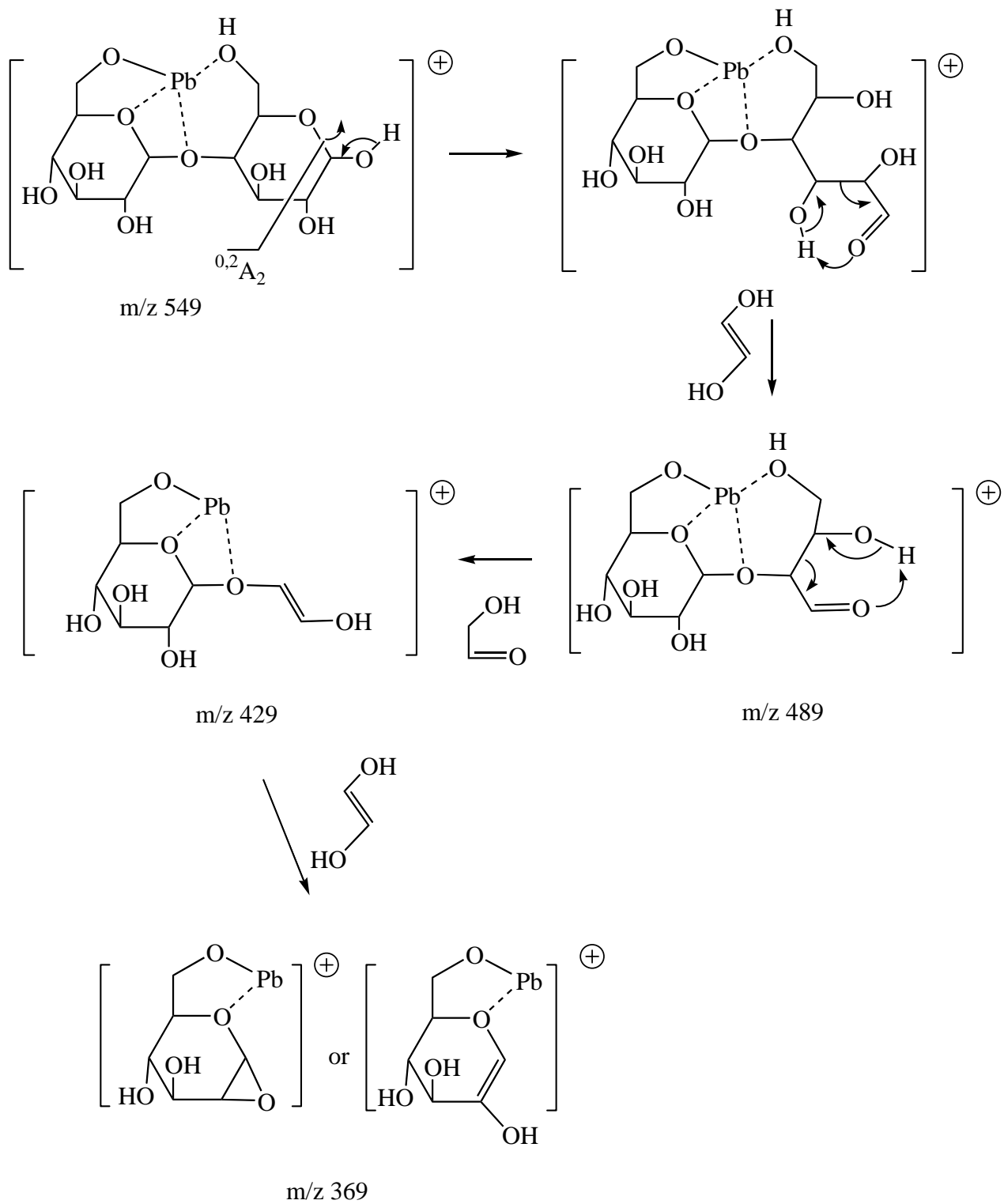
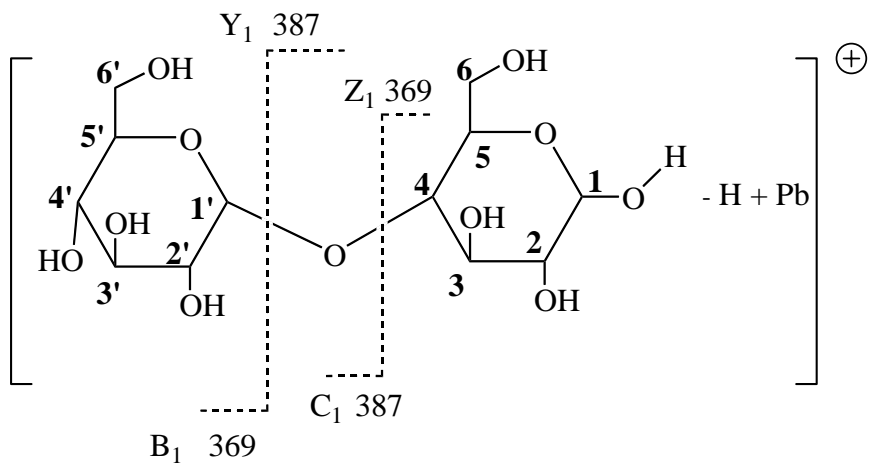


Figure 6



Scheme 1



Scheme 2